

The ESO Nearby Abell Cluster Survey^{*}

VI. Spatial distribution and kinematics of early- and late-type galaxies

P.A.M. de Theije and P. Katgert

Sterrewacht Leiden, Postbus 9513, 2300 RA Leiden, The Netherlands

Received 27 July 1998 / Accepted 30 September 1998

Abstract. Analysis of the data obtained in the ESO Nearby Abell Cluster Survey (ENACS) has shown that the space distribution and kinematics of galaxies *with* detectable emission lines in their spectra differ significantly from those of galaxies *without* emission lines. This result, and details of the kinematics, were considered as support for the idea that at least the spirals with emission lines are on orbits that are not isotropic. This might indicate that this subset of late-type galaxies either has ‘first approach’-orbits towards the dense core of their respective clusters, or has orbits that ‘avoid’ the core.

The galaxies with emission lines are essentially all late-type galaxies. On the other hand, the emission-line galaxies represent only about a third of the late-type galaxies, the majority of which do not show detectable emission lines. The galaxies without emission lines are therefore a mix of early- and late-type galaxies. In this paper we attempt to separate early- and late-type galaxies, and we study possible differences in distribution and kinematics of the two galaxy classes.

For only about 10% of the galaxies in the ENACS, the morphology is known from imaging. Here, we describe our classification on the basis of the ENACS spectrum. The significant information in each spectrum is compressed into 15 Principal Components, which are used as input for an Artificial Neural Network. The latter is ‘trained’ with 150 of the 270 galaxies for which a morphological type is available from Dressler, and subsequently used to classify each galaxy. This yields a classification for two-thirds of the ENACS galaxies.

The Artificial Neural Network has two output classes: early-type (E+S0) and late-type (S+I) galaxies. We do not distinguish E and S0 galaxies, because these cannot be separated very robustly on the basis of the spectrum. The success rate of the classification is estimated from the sample of 120 galaxies with Dressler morphologies which were not used to train the ANN. The success rate is higher for early-type than for late-type galaxies ($78 \pm 6\%$ vs. $63 \pm 6\%$). The weighted average success rate, irrespective of type, is $73 \pm 4\%$. The success rate is somewhat larger for the training set, and highest for the galaxies with emission lines.

Of the 3798 galaxies that were classified from their spectrum $57 \pm 7\%$ are of early type, and $43 \pm 7\%$ of late type. Using a subset of these 3798 galaxies, we constructed a composite cluster of 2594 galaxies, 399 of which have emission lines and are therefore almost exclusively spirals and irregulars. The kinematics and spatial distribution of the late-type galaxies *without emission lines* resemble much more those of the early-type galaxies than those of the late-type galaxies *with emission lines*. Yet, the late-type galaxies without emission lines may have a somewhat larger velocity dispersion and a slightly less centrally concentrated distribution than the early-type galaxies.

Only the late-type galaxies *with emission lines* appear to have a considerably larger global velocity dispersion and a much less concentrated projected density profile than the other galaxies. Thus, the suggestion of fairly radial, and possibly ‘first approach’ orbits applies only to spirals with emission lines. The early-type galaxies with emission lines (among which the AGN), may also have a large velocity dispersion and be concentrated towards the cluster centre.

Key words: galaxies: kinematics and dynamics – galaxies: clusters: general

1. Introduction

Recently, the kinematics of the different types of galaxies in clusters, as well as their spatial distribution, has received some new attention, e.g. from Colless & Dunn (1996), Carlberg et al. (1996) & Mohr et al. (1996). Generally speaking, the late-type galaxies are found to avoid the central regions of their clusters, while their line-of-sight velocity dispersion with respect to the average velocity of the cluster, σ_{los} , appears to be higher than that of the early-type galaxies.

The ESO Nearby Abell Cluster Survey (ENACS, Katgert et al. 1996, 1998) has yielded redshifts for more than 5600 galaxies in the directions of about 100 rich clusters of galaxies, mostly in a cone around the South Galactic Pole. Using the ENACS, Biviano et al. (1997, hereafter Paper III) compared the spatial distribution and kinematics of the galaxies with emission lines (hereafter: ELG) with those of the galaxies without emission lines (hereafter: non-ELG). From a subsample of 545 galaxies

Send offprint requests to: P. Katgert (katgert@strw.LeidenUniv.nl)

^{*} Based on observations collected at the European Southern Observatory (La Silla, Chile)

for which a morphological type is known, Biviano et al. concluded that the ELG are almost exclusively late-type galaxies, i.e., spirals (and irregulars), while the non-ELG are a mix of early- and late-type galaxies. They found that σ_{los} of the ELG is, on average, 20% larger than σ_{los} of the non-ELG, while the spatial distribution of the ELG is significantly less peaked towards the cluster centre than it is for the non-ELG. These two facts, in combination with details of the kinematics, were interpreted as evidence for a picture in which the ELG are mostly on fairly radial, ‘first approach’ orbits towards the central regions of their clusters, and thus not in full equilibrium with the population of non-ELG.

Biviano et al. estimated that the large majority of the ELG are spirals; however, the ELG appear to represent only about one-third of the total spiral population. Therefore, it was not clear whether the conclusion about the difference in kinematics of ELG’s applies only to spirals with emission lines, or whether it applies to all spirals. If the spirals among the non-ELG would have identical kinematics and spatial distribution as the spirals with emission lines, the real differences between early- and late-type galaxies would be larger than the apparent differences. That would bring the result of Biviano et al. more in line with that of Colless & Dunn (1996) who found that the velocity dispersion of the late-type galaxies in the main concentration of the Coma cluster is very close to $\sqrt{2}$ times that of the early-type galaxies.

On the other hand, it is conceivable that only the spirals with emission lines are on ‘first approach’ orbits, which would be consistent with the presence of sufficient amounts of line-emitting gas. The spirals without emission lines might then have traversed the central regions of their clusters and have lost most of their line-emitting gas in the process.

Recently, Ramírez & de Souza (1998) concluded that the orbits of elliptical galaxies in clusters are close to radial, while spirals have more circular shaped, or isotropic, orbits. Their conclusion is based on an analysis of the distribution of line-of-sight velocities.

In order to be able to investigate the kinematics of the spirals without emission lines, as well as to elucidate the cause for the apparent disagreement between the results of Ramírez & de Souza and that of Biviano et al., we need morphological types for the (non-ELG) galaxies in the ENACS. The obvious way to get these is through imaging. With well over 4000 galaxies without emission lines, that represents a major observational effort, on which we have embarked, but which will take some time to finish.

In this paper, we adopt a different approach, by using the ENACS spectra. The morphological types are estimated from the spectra with a Principal Component Analysis, in combination with an Artificial Neural Network. The network is ‘trained’ with a subset of the ENACS galaxies for which a morphological type is available from imaging (Dressler, 1980, hereafter D80) and it is ‘tested’ with the remaining galaxies with morphology from Dressler. With the morphological types estimated from the spectra, we investigate the kinematics and spatial distribution of, in particular, the late-type galaxies with and without emission lines.

The paper is organized as follows: in Sect. 2 the ENACS data is summarized. In Sect. 3 we describe the algorithm that we used to estimate the morphological type of a galaxy from its spectrum, by applying a PCA and an ANN. In Sect. 4 we discuss the results of the combined PCA/ANN and present the success rates achieved in assigning morphological types. In Sect. 5 we present an analysis of the spatial and kinematical differences between the (subsets of) early- and late-type galaxies. In Sect. 6 we summarize the results.

2. Data

In the present analysis we use the galaxy spectra obtained with the OPTOPUS instrument at the ESO 3.6m telescope at La Silla, Chile in the context of the ENACS. For a detailed description of the characteristics of the survey, we refer to Katgert et al. (1996, 1998). A brief summary of those aspects of the observations that are relevant to the analysis in this paper may be useful, however.

The observations were done between September 1989 and October 1993. The observed galaxies all lie in the direction of rich Abell clusters. The redshifts of these clusters are mostly ≤ 0.1 and most clusters lie around the South Galactic Pole in the solid angle defined by $b \leq -30^\circ$ and $-70^\circ \leq \delta \leq 0^\circ$. The galaxies were selected either on film copies of the SERC IIIa-J survey or on glass copies of the first Palomar Sky Survey. Areas of between 1 and 4 square degrees centered on the target clusters were scanned with the Leiden Astroscan plate-measuring machine. The magnitude limits are between 16.5 and 17.5 in the R-band (see Katgert et al. 1998 for details). These limits correspond to absolute magnitudes of -19.8 and -18.8 at the median redshift $z = 0.06$ of the survey, assuming a Hubble parameter of $100 \text{ km s}^{-1} \text{ Mpc}^{-1}$.

The OPTOPUS system used fibres with a diameter of 2.3 arcseconds, which corresponds to a linear scale of $2.1 h^{-1} \text{ kpc}$ at a redshift of $z = 0.06$. In 6 of the 9 observing runs the same spectrograph setup was used. In general, the wavelength range was from $\approx 3850 \text{ \AA}$ to $\approx 6000 \text{ \AA}$, but it varies slightly between runs. The spectral resolution is almost always 130 \AA/mm , or about 5 \AA , except in the run of September 1989, which has a lower resolution. Due to different pixel sizes of the CCD detectors used, the spectra were sampled at either 1.9 or 3.5 \AA/pixel .

In the wavelength range covered by the observations, and for the redshifts of the clusters observed, the principal emission lines that were observable are [OII] (3727 \AA), $H\beta$ (4860 \AA) and the [OIII] doublet (4959 and 5007 \AA). Possible emission lines were identified independently by two persons: in the 2-D frames and in the 1-D extracted spectra (see Paper III for details). In the spectra of about 1200 galaxies one or more emission lines were detected. For 554¹ galaxies in the 10 ENACS clusters in common with the sample of Dressler (1980) the morphology is available. Of the 71 ELG which have a morphological classification in D80, 61 are spirals or irregulars (86%), 8 are S0’s (11%) and 2 are ellipticals (3%). On the other hand, of the 181

¹ This number is slightly larger than the number mentioned in Paper III (which was 545), due to an updated cross-reference between the ENACS sample and the Dressler catalogue.

spirals that the D80 set has in common with ENACS, 61 show emission lines. So, while 6 out of 7 ELG are spirals/irregulars, only 1/3 of the spirals are ELG. A small fraction (about 7% according to Biviano et al. 1997) of the ELG are active galactic nuclei, as is evident from the line widths.

The spectra that were obtained in September 1992 often exhibit peculiarities, such as deviant pixels at beginning and end of the spectrum. These probably were introduced in the reduction process and have not influenced the redshift determination. We have not reduced these spectra again for the present analysis, but we have excluded them from the analysis, as they could produce below-average classification results (see Sect. 4.2).

3. Spectral classification

For the classification of the galaxies on the basis of their spectrum, we use a two-step scheme in which we first describe a spectrum in terms of its most significant Principal Components (PCs), and then use a trained Artificial Neural Network to classify the galaxy on the basis of those components. In this section, we summarize the methods that we used and the details of their implementation as far as those are required for an appreciation of the results.

Several authors applied PCA (either by itself or in combination with an ANN) to the problem of trying to determine from a spectrum the stellar or galaxy type. Deeming (1963), in classifying stellar spectra, found a very good correlation between the first, most important PC and the stellar type. Francis et al. (1992) carried out a study of a large sample of QSO spectra, and developed a classification scheme based on the first three PCs. Von Hippel et al. (1994) used an ANN to classify stellar spectra and concluded that they could recover the stellar type to within 1.7 spectral subtypes. Sodr e Jr. & Cuevas (1994) showed that the spectroscopic parameters extracted from the spectra of galaxies, like the amplitude of the 4000   break or of the CN band, correlate well with Hubble type.

Zaritsky et al. (1995) decomposed galaxy spectra into an old stellar component, a young stellar component and various emission-line spectra. They classified the galaxies by comparing the relative weights of the components with those of galaxies of known morphological type and found that the spectral classification agreed with the morphological classification to within one type (e.g. E to S0 or Sa to Sb) for $\geq 80\%$ of the galaxies. Connolly et al. (1995) decomposed each spectrum into eigenspectra and found that the distribution of spectral types can be well described by the first two eigenspectrum coefficients.

Folkes et al. (1996) combined PCA and ANN to classify galaxy spectra. Their purpose was to investigate galaxy classification from spectra to be obtained in the 2dF Galaxy Redshift Survey. They generated artificial spectra and obtained a success rate of more than 90% in recovering the galaxy type from the spectrum.

Lahav et al. (1996) used ESO-LV galaxies (Lauberts & Valentijn 1989) and grouped them in three ways. From a PCA applied to 13 galaxy parameters they found that different morphological types occupy distinct regions in the plane defined by

the two most important PCs. They also used an ANN with the 13 galaxy parameters as input and concluded that with a single output node, there is a strong correlation between the galaxy type indicated by the ANN-output and the input type. Using two output nodes, one for early- and one for late-type galaxies, the overall success rate was 90%, which decreased to 64% if 5 output nodes were used, viz. E, S0, Sa+Sb, Sc+Sd and I.

In the last few years several more applications of PCA analysis, combined PCA and ANN analysis, or ANN analysis were published. In the field of stellar classification see e.g. Bailer-Jones (1997), Iбата & Irwin (1997), Weaver & Torres-Dodgen (1997) and Singh et al. (1998), and in the area of galaxy classification e.g. Galaz & de Lapparent (1998) and Bromley et al. (1998).

3.1. Principal component analysis

Principal Component Analysis (PCA) is a technique developed for data compression as well as data analysis. As measured parameters, like e.g. spectral fluxes, may be correlated, it is of interest to determine the minimum number of *independent* variables that can describe the larger amount of correlated observed parameters. A full description of PCA can be found in e.g. Kendall & Stuart (1968) and Folkes et al. (1996). In our analysis, the PCA is an important first step as it reduces the number of parameters that describe the galaxy spectrum, while it recovers essentially all significant information and reduces the noise.

3.1.1. Preparing the data

Before we could apply PCA to the ENACS galaxy spectra some preparations were necessary. First, all spectra were inspected and a few spectra with strong discontinuities or other non-physical features were discarded. Secondly, sky lines were removed by linear interpolation. Thirdly, the spectra were shifted back to zero-redshift and corrected for the response functions of the OPTOPUS instrument (spectrograph and CCD detector). Fourthly, a maximum common (zero-redshift) wavelength range had to be established for as large a subset of the galaxy sample as possible.

Using all galaxies in the ENACS survey, this common wavelength range would be rather small because background galaxies have redshifts up to $z \approx 0.15$. We have chosen to use the zero-redshift wavelength range from $\lambda_{min} = 3720$   to $\lambda_{max} = 5014$  . This range includes all 4 major emission lines (see Sect. 2) and provides at least 7   continuum beyond the [OII] 3727   and [OIII] 5007   lines. All spectra were resampled in the range $[\lambda_{min}, \lambda_{max}]$ with $\Delta\lambda/\text{pixel} = 3.5$  , which yields 371 spectral fluxes.

For some field galaxies the zero-redshift spectrum did not fully cover the wavelength range $[\lambda_{min}, \lambda_{max}]$. When the wavelength coverage of a galaxy spectrum fell short by more than 70   (i.e., 20 pixels) from the $[\lambda_{min}, \lambda_{max}]$ interval, the galaxy was removed from the sample. When the galaxy spectrum fell short by less than 70  , it was extrapolated by a second-order

polynomial either down to λ_{min} or up to λ_{max} , or both. This extrapolation does not introduce major errors in the fluxes at the edges of the spectrum.

Finally, the spectra were normalized to unit integral. For the normalization we interpolated the spectrum in the regions of 20 Å centered on the emission lines because a strong emission line may result in a continuum which is too low.

Leaving out all spectra that were observed in September 1992 and rejecting all galaxies for which more than 20 pixels had to be added at either one or both ends to fill the spectral range $[\lambda_{min}, \lambda_{max}]$, we retained 3798 galaxies for the PCA. For 270 of these, a morphological classification is available from D80.

3.1.2. Determining the principal components

After the preparation described in Sect. 3.1.1 the resampled spectrum of each galaxy defines a j -dimensional vector \mathbf{x} , whose components represent the flux in the j pixels of the spectrum, with $j = 1-371$. From each component x_j we subtract the mean over all galaxies, \bar{x}_j , to centre the j -th parameter on zero (remember that we normalized all spectra to the same integral of 1.0). The values $x_j - \bar{x}_j$ can be used in two different ways in the PCA. Firstly, $x_j - \bar{x}_j$ may be normalized by its standard deviation σ_j . In that case, each of the components of the spectral vectors has unit variance for the set of spectra used. This method is sometimes recommended as it puts each input parameter on a similar scale. In this way, one may construct vectors from components that are not related, such as e.g. mass and size.

However, there are cases in which the different dispersions or the relative strengths of the inputs are important (see e.g. Folkes et al. 1996). E.g., in our PCA the components of the spectral vectors that contain the principal emission lines will have a larger variance, as these may or may not be present, and it may be important to retain this information. We did the PCA with and without normalization with the standard deviation, and obtained better results with normalization than without.

The PCA solves for the weights w_{kj} that define the 371 PCs e_k which follow from the spectral fluxes by the relation: $e_k = \sum_{j=1}^{371} w_{kj}(x_j - \bar{x}_j)/\sigma_j$. The PCs are thus linear combinations of the normalized spectral fluxes and form an orthogonal basis. The first PC, e_1 , contains most of the variance between the spectra and describes the most characteristic difference between the spectra. The last PC contains least of the variance and will be most affected by noise. In practice, we have restricted the ANN analysis to the 15 most significant PCs (see Sect. 4.2).

In Fig. 1 we show two examples of spectra and their PCA reconstruction, based on the first 15 PCs. These examples illustrate that the spectra can be reconstructed quite well with only a limited number of PCs. There may be some indication that the spectrum of an elliptical is easier to represent with 15 PCs than that of a spiral, but the difference is slight.

3.1.3. Physical meaning of the PCs

In Fig. 2 we show the average spectrum of the 3798 galaxies in the data set, together with the weights for the 3 most significant

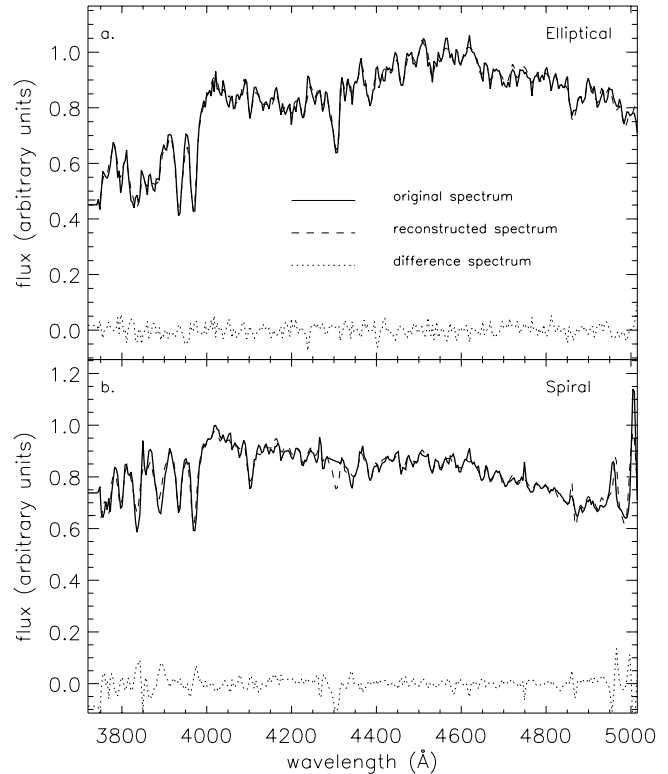


Fig. 1a and b. Comparison of two ENACS spectra with the reconstruction of the same spectra from the first 15 Principal Components. The solid line is the observed galaxy spectrum, the dashed line is the reconstructed spectrum. The dotted line indicates the difference between the observed and the reconstructed spectrum. **a** Elliptical galaxy, **b** Spiral galaxy.

PCs, i.e., w_{1j} , w_{2j} and w_{3j} . The weights for the first PC, w_{1j} , indicate that e_1 represents the colour of the galaxy, as it measures the flux in the interval $\lambda = [3720, 4350]$ Å minus the flux in the interval $\lambda = [4350, 5120]$ Å. The wavelength dependence of w_{1j} is very similar to that in Sodr  & Cuevas (1997, their Fig. 5). The second PC, with weights w_{2j} , apparently measures the curvature of the spectrum, i.e. the flux between $\lambda = 4000$ Å and $\lambda = 4600$ Å, minus the flux below and above these wavelengths. The weights for the third PC, w_{3j} , have a signature just redwards of the 4000 Å break, and e_3 thus seems to be sensitive to the strength of this break. Sodr  & Cuevas (1994) noted that the 4000 Å break correlates well with Hubble-type. The third PC also appears to weigh the G-band at $\lambda \approx 4300$ Å. It gets progressively more difficult to understand in detail the physical meaning of the higher order PCs, but they gauge the various less conspicuous features in the spectrum, such as the many absorption and emission lines.

Note that we expressed the PCs in terms of the spectral data, which provides an immediate physical meaning of the weights w_{ij} . In an alternative but fully equivalent representation, the spectral data can be approximated by a weighted sum of eigenspectra; see e.g. Connolly et al. (1995) or Galaz & de Lapparent (1998).

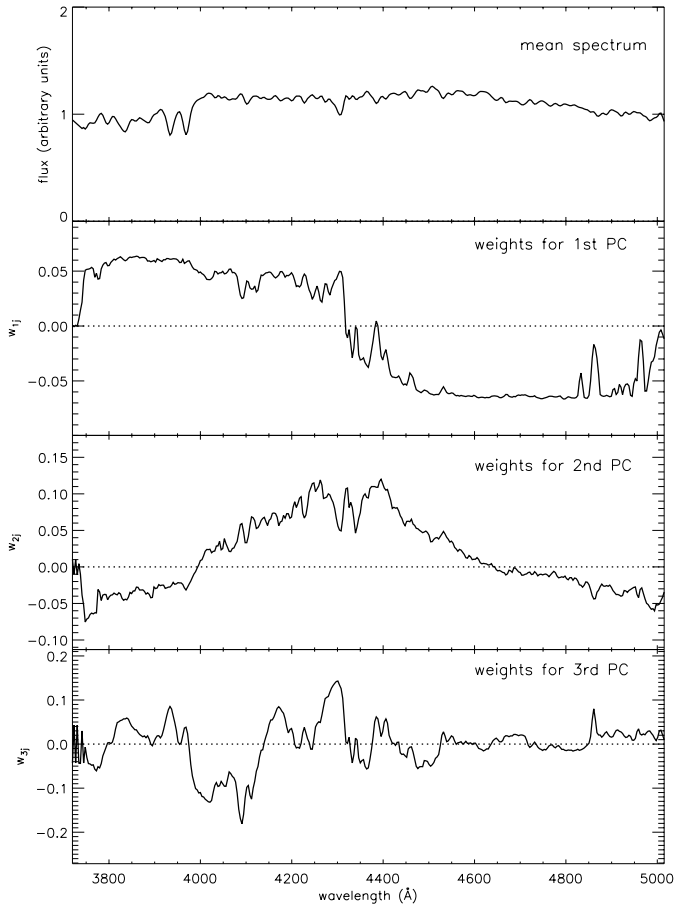


Fig. 2. Average galaxy spectrum, and the weights w_{ij} for the first 3 Principal Components ($i=1-3$), calculated for the entire data set of 3798 galaxies. See text for more details.

3.2. Artificial neural networks

The first 15 PCs derived for each spectrum are used as input for an Artificial Neural Network (ANN). The ANN determines the optimum way of combining the PCs in order to obtain a single number which maps, with maximum discriminating power, onto the desired quantity which, in our case, is morphological type. ANNs are frequently used to recognize patterns in input data. An array of parameters is presented as input to the ANN, which must have been trained to recognize the desired patterns. The ANN then yields the class of object for which the input array is most characteristic. The classification is objective: the ANN is true to the training it received, and repeatable.

An ANN uses weights to translate the input data into one or more parameters which can be compared with the corresponding parameters for the training set in order to estimate the class of an object. The weights in the ANN are determined by an iterative least-squares minimization using a back-propagation algorithm. In each iteration step, the current values of the weights are updated according to the difference between the supplied output type and the calculated output type. For a full description of ANNs, the reader is referred to e.g. Hertz et al. (1991), Kröse & van der Smagt (1993) and Folkes et al. (1996).

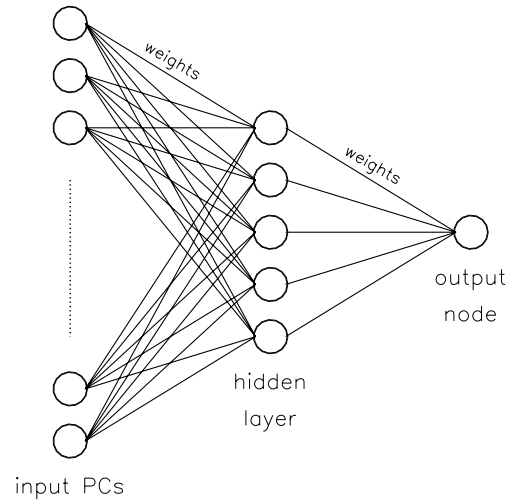


Fig. 3. Schematic diagram of the Artificial Neural Network that we used. The network determines the galaxy type ('output node'), from the Principal Components describing the galaxy spectrum. Each node in a given layer is connected to all nodes in the adjacent layers by weight vectors.

3.2.1. Training the ANN and tuning its parameters

We trained the ANN by using the spectra of 150 of the 270 galaxies in our sample of 3798 for which Dressler (1980) gives a morphological type. The median redshift of the clusters studied by Dressler is about 0.04, which is significantly smaller than the median redshift of the ENACS sample of about 0.07. The 10 clusters in common between D80 and ENACS have redshifts between 0.04 and 0.07. The training set contains approximately equal numbers of galaxies in each of the three morphological classes that we attempted to 'resolve', viz. E, S0 and S+I.

The complexity of an ANN depends strongly on the number of inputs per galaxy and on the number of hidden nodes, layers, outputs, and connections. Therefore, one is well advised to use as few of these as possible (de Villiers & Barnard 1993), as long as the discriminating power of the ANN is not affected. For that reason, only the 15 most significant PCs of the galaxy spectra were presented to the ANN, rather than all 371 original spectral fluxes. By using only the 15 most significant PCs, we also reduce the noise considerably, as the latter is mostly contained in the higher-order PCs.

We used only one hidden layer, which contains 5 nodes. This makes the backpropagation network much more rapid to train (see e.g. de Villiers & Barnard 1993).

Only one output node was used, with output values in the interval $[0,1]$. Some authors define a separate output node for each of the morphological types that can be assigned to the galaxies (e.g. Storrie-Lombardi et al. 1992). The output node which has the highest 'activity' then determines the galaxy morphology. However, because galaxies are thought to form a continuous instead of a discrete sequence of different morphologies (e.g. Naim et al. 1995), we have chosen to describe the sequence with only one output node with a continuous range of output values. A schematic diagram of the ANN we used is shown in Fig. 3.

When training the ANN, it is essential to stop the iterative minimization at the right moment. One option is to stop when the total error between calculated output types and supplied output types of the *training set*, the so-called ‘cost function’, drops below a certain value, or changes little between successive iteration steps. However, this may result in ‘over-fitting’, i.e., one may interpret the statistical fluctuations in the training set as global characteristics. Another option is to minimize the cost function as calculated for the *test set* (Lahav et al. 1996). Because the ANN is not trained on this set, the cost function will usually have a true minimum at a certain iteration step, and increase after that. In our case the results are almost identical for both options.

As we want to extend the analysis in Paper III to early- and late-type galaxies, we are primarily interested in a two-class classification. Therefore, we trained the ANN for a pure early-/late-type division which allows a separation of the heterogeneous class of non-ELG into early- and late-type galaxies. An additional reason for taking ellipticals and S0’s together in one class was given by Lahav et al. (1996), who found that 76% of all early-type galaxies were correctly classified by their ANN, but that of the S0’s only 66% was classified correctly. They suggested that this may be an indication that the S0’s form a ‘transition class’ in the Hubble sequence. Sodr  & Cuevas (1997) found that the first, most significant PC of ellipticals and S0’s are very similar, so it is hard to distinguish between them on the basis of their spectrum.

We have also trained the ANN for a three-class division into E, S0 and S+I. We defined the output values of the ANN for these three classes to be 1/6, 1/2 and 5/6. In principle, we could have defined different output values for these three categories which would have resulted in different weights in the trained ANN. However, we find that an ANN with output values of 0, 1/2 and 1 gives classification results that are essentially identical to those obtained with the output values 1/6, 1/2 and 5/6. Galaxies are assigned the morphological classification for which the difference between their ANN output parameter and the output parameter defined for the class is smallest. After running the three-class ANN we also sum the E and S0 categories to produce the equivalent of the early-type category in the two-class ANN. We find that there are no significant differences between the results of a true two-class ANN and a semi two-class ANN obtained by combining the E and S0 classes in a three-class ANN. Below we will describe the results for the latter.

3.2.2. Testing the ANN

In addition to training the ANN, we tested it with a test set consisting of the remaining 120 galaxies with morphology from D80. The results for this test set, in terms of the success in classifying the galaxies correctly, are valid for the entire data set of ENACS galaxies for which no morphological classification is available. However, for the latter we do have information on the presence or absence of detectable emission lines in the ENACS spectrum, and we will use that to refine the determination of the

ANN output parameter which best separates early- and late-type galaxies.

3.2.3. Optimizing the classification results

Our goals are to optimize the success rate of the classification, to obtain the observed fraction of late-type galaxies among the ELG (viz. 86%, see Paper III), and to obtain the correct fractions of E, S0 and S+I galaxies used to train and test the ANN. The only freedom one has to achieve these goals, after tuning all parameters as described in Sect. 3.2.1, is to set the output ranges within which a galaxy will be classified as E, S0 or S+I. A priori, the most logical choice the output ranges is [0,1/3], [1/3,2/3], and [2/3,1] for E, S0 and S+I, respectively. However, we find that the ranges [0.00,0.34], [0.34,0.59] and [0.59,1.00] produce a fraction of early-type galaxies among the ELG that is more consistent with observations than that found with the a priori choice. In the following we will therefore use the ranges [0.00,0.34], [0.34,0.59] and [0.59,1.00]. Note, however, that the success rates for the two sets of output ranges differ by at most a few percent.

3.3. Possible causes of misclassification

There are a number of factors that determine the performance of the classification algorithm.

First, the representation of the spectra by the first 15 PCs is not perfect. However, the error one makes if one only uses the first 15 PCs is probably quite small (see Fig. 1), while the results are not expected to depend much on the exact number of PCs used, as long as this number is large enough (see also Sect. 4.2). On the other hand, it is likely that the correspondence between the characteristics of the spectrum (as quantified in the first PCs) and the morphology is not entirely one-to-one. For instance, the spectrum of a late-type galaxy is likely to depend on the location in the galaxy; viz., if the aperture of the spectrograph covered only the central region of such a galaxy, a significant contribution of a bulge may well create an apparent inconsistency between morphological and spectral classification.

Secondly, morphological classification is not easy. For example, it is likely that some S0 galaxies, especially those seen face-on, are classified as ellipticals, on the basis of the image only (this is less likely if the brightness profile is used as well). On the other hand, edge-on S0 galaxies and spirals are not always easy to classify correctly. Naim et al. (1994) showed that there is indeed some ambiguity in classifying galaxies solely on the basis of the morphology of the images. They found 6 experts willing to classify a set of 831 galaxy images. The results show that both types of disagreement mentioned above do indeed occur, as well as differences in the verdict of whether a spiral galaxy is of early or late type. The *r.m.s.* differences between verdicts of experts ranged from 1.3 to 2.1 Revised Hubble types. This is as large as the *r.m.s.* dispersion between the *mean classification* of the 6 experts on the one hand and the results of an ANN analysis on the other (Naim et al. 1995).

Table 1. Distribution of morphological type for the galaxies that Dressler (1980) classified twice, in the cluster DC 0326–53 as well as in DC 0329–52. The last column and the bottom line of each half of the table indicate the fraction of galaxies that is classified into the same class twice.

Three-class system				
	E	S0	S+I	%
E	15	1	0	0.94
S0	3	11	2	0.69
S+I	1	1	6	0.75
%	0.79	0.85	0.75	

Two-class system			
	E/S0	S+I	%
E/S0	30	2	0.94
S+I	2	6	0.75
%	0.94	0.75	

Even an expert is not always totally consistent. Using the 40 galaxies in Dressler’s catalogue that were classified twice, once in the cluster DC 0326–53 and once in DC 0329–52, this effect can be quantified. A comparison between both classifications of D80 is given in Table 1. In the three-class system, 8 out of the 40 galaxies have an inconsistent classification, and at least 4 of the 40 classifications (or 10%) are thus incorrect. In addition, it cannot be excluded that galaxies for which both independent classifications are identical, have yet been classified incorrectly; so, the 10% of misclassifications is a lower limit. If one takes E and S0 galaxies together to obtain an early- vs. late-type classification, the number of misclassifications is at least 5%. Note, however, that the other way to read this number is that D80 is close to 95% consistent: an impressive achievement, as will be confirmed by anybody who has done morphological classification.

Thirdly, as mentioned before, the spectral difference between E and S0 galaxies probably is not very large (see Lahav et al. (1996) and Sodr e & Cuevas (1997)).

Fourthly, Zaritsky et al. (1995) found that for 51 of the 304 galaxies in their sample (i.e. for 17%) the spectral typing is not consistent with the morphological classification to within one morphological type (E, S0, Sa, Sb, Sc and Irr). In 36 cases there is a discrepancy between morphological and spectral classification that transgresses the early-/late-type galaxy boundary. It is noteworthy that there are 16 cases of early-type morphology with late-type spectrum (mostly on the basis of emission lines), and 20 cases of late-type morphology with early-type spectrum. I.e. the effects of misclassification appear to be more or less symmetric, and can therefore be considered as sources of random errors, like the effects mentioned above.

For several hundred of the ENACS galaxies that we studied in this paper and for which we obtained a spectral classification, we also have obtained CCD images which yield a morphological classification. Provisional results indicate that for our spec-

tral classification method, the misclassification probably is not symmetric between early-type morphology/late-type spectrum confusion and vice versa (Thomas & Katgert, in preparation). Only 10% of the E and E/S0 galaxies in our sample have a >50% probability that their spectrum is late-type. For the S0 galaxies this fraction increases to about 20%. However, about 30% of the spiral galaxies has a spectrum that has a >50% chance of being indicative of an early-type galaxy. This suggests that the chance of a spectral misclassification of an early-type galaxy is considerably smaller than that of a spectral misclassification of a late-type galaxy. Presumably, the fact that the ENACS spectra sample only the central few kpcs of the galaxies, amplifies the influence of the bulges on the spectral classification of late-type galaxies.

3.4. Dependence of results on algorithm parameters

A number of choices were made and parameters were chosen in our classification algorithm. The first one is the number of PCs that is used in the ANN. In principle, this number is important, as using too few components to describe the spectrum will make the fits to the original spectra less accurate. The ANN will then have more problems to classify the galaxies. If one uses too many components, one may model the spectra too precisely and use PCs which are too noisy. In Sect. 4.2 we will check how the results depend on the number of PCs.

If one does not normalize the spectral fluxes to unit variance (see Sect. 3.1.2), the relative strengths of the spectral points are retained. This may be important (FLM96) and it emphasizes certain emission or absorption lines. If we do not normalize to unit variance, the success rates are smaller than when all pixels are normalized to unity. Sodr e & Cuevas (1997) also mention that the spread in the first two PCs is larger if the input parameters are all normalized to unit variance.

The exact number of nodes in the hidden layer of the ANN is of minor importance. Using 5 or 7 nodes gives essentially the same results, but using only 3 nodes produces results that are slightly worse. The exact values of the learning parameters and the weight–decay term of the ANN (see e.g. Kr ose & van der Smagt 1993) are not important either, as long as they are sufficiently small, i.e., 0.001–0.01. The number of cycles through the input list of training galaxies that is needed, however, does depend on the values of the learning parameters.

The number of galaxies used to train the ANN is not critical, as long as it is sufficiently large, say 150. However, the *r.m.s.* values around the average classification result (see Sect. 4.2) may depend on the number of galaxies in each of the morphological classes. The number of galaxies with which we have chosen to train the ANN, viz. 150, is a compromise between having a sufficient number of galaxies to train the ANN, and having enough galaxies left to test the performance of the ANN. It is important, however, that all three main morphological types are represented in the training set with roughly equal numbers. If one morphology is overrepresented with respect to the other types in the training set, there will be a positive bias for that particular type. So, in principle, the composition of the training

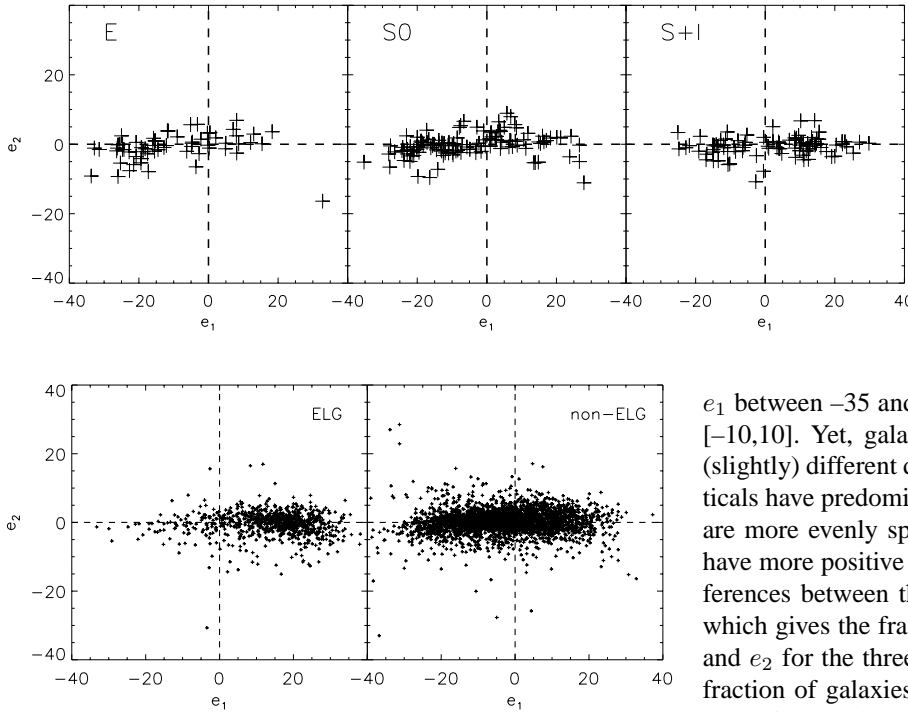


Fig. 4. Distribution with respect to the first and second Principal Components, e_1 and e_2 , for galaxies of type E (62 galaxies), S0 (118) and S+I (90), as classified by D80.

Fig. 5. Distribution with respect to the first and second Principal Components, e_1 and e_2 , for emission-line galaxies (ELG, 808 galaxies) and galaxies that do not show emission lines (non-ELG, 2990 galaxies).

Table 2. Distribution with respect to the first and second Principal Components, e_1 and e_2 . In the upper half of the table the galaxies are grouped according to morphology (from D80). In the lower half, galaxies are grouped according to the presence (ELG) or absence (non-ELG) of emission lines.

type	N	$\%(e_1 > 0)$	$\%(e_2 > 0)$
E	62	24	40
S0	118	36	45
S+I	90	61	39
ELG	808	87	46
non-ELG	2990	39	52

set should closely mimic the composition of the sample to be classified in order to have minimum bias.

4. Results

4.1. Segregations in PCA-space

The PCA is completely ‘self-propelled’, i.e., it does not need to be tuned or trained. Therefore it is interesting to look at the results of the PCA for the galaxies with morphology from D80, as well as for the galaxies with and without emission lines, to see in what way the PCs and the morphology or emission-line character correlate.

In Fig. 4 we show, for all 270 galaxies with morphology from D80, the distribution with respect to the first and second PCs for the 3 classes E, S0 and S+I. All galaxies have values of

e_1 between -35 and 35 while e_2 is almost always in the range $[-10, 10]$. Yet, galaxies of different morphological type have (slightly) different distributions in the (e_1, e_2) -plane. The ellipticals have predominantly negative values of e_1 , the lenticulars are more evenly spread in e_1 while the spirals and irregulars have more positive values of e_1 than negative ones. These differences between the distributions are quantified in Table 2, which gives the fraction of galaxies with positive values of e_1 and e_2 for the three morphological classes. It is clear that the fraction of galaxies with $e_1 > 0$ increases towards later type. There is a tendency for e_2 to be slightly negative on average, although the effect is not very significant in view of the statistics. As the information content of the PCs e_i decreases with increasing i , the higher-order PCs will not have, by themselves, more discriminating power than e_2 .

The effect visible in Fig. 4 and Table 2 is qualitatively similar to that found by Lahav et al. (1996) who used 13 galaxy parameters (e.g. blue minus red colour, central surface brightness) and found that different morphological types occupy distinct regions in the (e_1, e_2) -plane. They even detected a slight separation between E and S0 galaxies, although the regions occupied by the two morphological types had considerable overlap.

In Fig. 5 we show the distribution with respect to the first and second PC for the ELG (lefthand panel) and the non-ELG (righthand panel). There is a clear difference between the two distributions, with almost 90% of the ELG having a positive value of e_1 , while the non-ELG have, on average, a slightly negative value of e_1 (see also Table 2). Qualitatively, Figs. 4 and 5 are quite consistent, in view of the fact that almost all ELG are spirals (see Paper III). It is interesting to note that apparently the ELG represent those spirals that have essentially only positive values of e_1 .

Note also that the difference between ELG and non-ELG persists if we do not include in the PCA the spectral ranges where the main emission lines can occur. This shows that it is not only the emission lines themselves which distinguish ELG from non-ELG, but that more global properties of the spectrum, such as continuum slope (see Sect. 3.1.3), correlate with the presence of emission lines.

4.2. Success rates

In Table 3 we give the results of our morphological classification using the ANN operating on the 15 most significant PCs. The

Table 3. Success rates (in percentages) for classifying galaxies with the ANN. The numbers are averages ($\pm r.m.s.$ values around these averages) over 10 realizations of the ANN. For each realization, different sets of galaxies (which are partly correlated) are used to train the ANN. The first column gives the galaxy type as classified by D80. The second column gives the number of galaxies of this type that is used in the training set. The third, fourth and fifth columns give the fraction of galaxies (per morphological type) that is labeled as E, S0 and S+I, respectively, in the training set by the ANN. Column 6 gives the number of galaxies in the test set. Columns 7 to 9 give the fraction of galaxies (per morphological type) that is labeled as E, S0 and S+I, respectively, in the test set by the ANN. In the lower half of the table, the E and S0 galaxies are combined.

Three-class system								
type	Training set				Test set			
	N	%E	%S0	%S+I	N	%E	%S0	%S+I
E	53 \pm 3	53 \pm 19	45 \pm 19	2 \pm 2	9 \pm 3	34 \pm 28	50 \pm 24	16 \pm 12
S0	55 \pm 3	13 \pm 8	68 \pm 10	19 \pm 6	63 \pm 3	23 \pm 11	49 \pm 15	28 \pm 7
S+I	55 \pm 3	1 \pm 1	18 \pm 6	81 \pm 5	34 \pm 3	13 \pm 7	24 \pm 8	63 \pm 6

Two-class system						
type	Training set			Test set		
	N	%E+S0	%S+I	N	%E+S0	%S+I
E/S0	108 \pm 5	90 \pm 3	10 \pm 3	72 \pm 5	78 \pm 6	22 \pm 6
S+I	55 \pm 3	19 \pm 5	81 \pm 5	34 \pm 3	37 \pm 6	63 \pm 6

percentages quoted are averages ($\pm r.m.s.$ values around these averages) over 10 realizations of the ANN. For each realization, different sets of galaxies (which are thus partly correlated) are used to train the ANN. We give this information for the *test set* as well as for the *training set*. We consider two cases: the three-class ANN classification (top), and its compressed pseudo two-class version obtained by combining the E and S0 classes of the three-class classification (see Sect. 3.2.1).

The overall success rates for the training and test sets are $67 \pm 5\%$ and $49 \pm 6\%$, respectively, for the three-class system, giving each of the three classes equal weight. The success rate for the training set is larger than for the test set, which must be due to the fact that the ANN weights are calculated using the galaxies in the training set only. The success rate for the test set, however, is the one that should be applied to the entire set of galaxies to be classified.

If one uses the two-class system, viz. separating between early- and late-types only, the success rate for the training set is $87 \pm 3\%$ and for the test set $73 \pm 4\%$. Obviously, these success rates are larger than for the three-class system because one has less categories to classify the galaxies in, and because a large fraction of the classification ‘failures’ occurs between E’s and S0’s. The fact that in the two-class system the success rate of the early-type galaxies is higher than for the late-type galaxies may be due, at least partly, to the asymmetry between early- and late-type galaxies in our spectral misclassifications, as discussed in Sect. 3.3.

Using the galaxies classified by Dressler, we determined how the spirals that are incorrectly classified are distributed between early- and late-type spirals. For the training set, only 30% of the spiral galaxies that are classified as S0 by our ANN are of type Sb or later, according to D80. Sodr e & Cuevas (1997) obtained a similar result, namely that the spectral variation, as measured by the first PC, is slow from E to Sab and increases

strongly for later types. So one expects few Sb or later-type spirals to be classified as early-type. For the test set, all spirals classified as E by the ANN are of type Sa. For the training set 30% of the spirals of type Sa, 10% of type Sb, 13% of type Sc and 0% of type Sd+I are classified incorrectly. For the test set, these numbers are 26% for Sa, 13% for Sb and 0% for Sc or later. The early-type spirals are thus more often misclassified as E or S0 than the late-type spirals.

The fraction of the 808 ELG in the ENACS sample, used in the present analysis, that is classified as E, S0 or S+I is $7 \pm 5\%$, $13 \pm 4\%$ and $80 \pm 7\%$, respectively. Biviano et al. found that out of the 71 ELG with a morphological type available, 86% are of type S+I, 11% are S0 and 3% are elliptical. The fraction of ELG that is classified as spiral (80%) is higher than would be expected from the individual success rates for the E, S0 and S+I subsamples (Table 3) and the distribution of ELG over morphological type (Paper III). These would imply that $[0.03 \times (16 \pm 12)] + [0.11 \times (28 \pm 7)] + [0.86 \times (63 \pm 6)] = 58 \pm 5\%$ of the ELG would be classified as a spiral. Apparently, the success rate for the ELG is larger than for the entire data set containing both ELG and non-ELG, which could imply that ELG are preferentially *late* spirals, for which the classification is more reliable than it is for early spirals.

Based on the results of Table 3 one expects 59 ± 32 E’s, 110 ± 35 S0’s and 100 ± 9 S+I galaxies in the set of 270 ENACS spectra with a classification by D80. These numbers agree very well with the actual numbers in the D80 set, viz. 62 E’s, 118 S0’s and 90 S+I. However, this is not too surprising, as the correspondence between both sets of numbers was one of our criteria to set the output ranges (Sect. 3.2.3).

The distribution of galaxy types for the entire sample of 3798 spectra in our final sample is: $24 \pm 5\%$ E, $33 \pm 4\%$ S0 and $43 \pm 7\%$ S+I.

Table 4. Success rates (in percentages) for classifying galaxies with the ANN using different numbers of Principal Components (PCs). The numbers are averages ($\pm r.m.s.$ values around these averages) over 10 realizations of the ANN. For each realization, different sets of galaxies (which are partly correlated) are used to train the ANN. The results are given for the training and test sets separately and both for the three-class and the two-class classification systems.

Training set			
system	10 PCs	15 PCs	20 PCs
three-class	62 \pm 4	67 \pm 5	69 \pm 4
two-class	85 \pm 2	87 \pm 3	86 \pm 3
Test set			
system	10 PCs	15 PCs	20 PCs
three-class	43 \pm 7	49 \pm 6	48 \pm 6
two-class	68 \pm 13	73 \pm 4	70 \pm 6

Of all AGN in our sample, $55 \pm 10\%$ is classified as early-type. This is significantly more than the $20 \pm 7\%$ of *all* ELG that is classified as early-type. Apparently, there are significantly more early-type galaxies among AGN than there are among the non-AGN ELG.

In Table 4 we give the success rates for the galaxy classification if one uses different numbers of PCs. It appears that the results obtained with 10 PCs in the ANN may be marginally worse than those with 15 or 20 PCs, but the differences are not very significant.

We have also run the PCA and ANN with the spectra of the September 1992 period included as well. The classification results then are $63 \pm 3\%$ (three-class) and $83 \pm 2\%$ (two-class) for the training set, and $44 \pm 3\%$ (three-class) and $69 \pm 2\%$ (two-class) for the test set. These success rates are slightly lower than those if the spectra from the September 1992 period are not included, and they justify our choice not to include those galaxies in the analysis.

Finally, we have investigated if the success rates depend clearly on the S/N-ratio of the galaxy spectrum. This is not the case, as is expected because, by construction, the first PCs will contain relatively little noise.

5. Spatial and kinematical differences between early- and late-type galaxies

Biviano et al. (1997) studied the differences between ELG and non-ELG as far as their spatial distribution and kinematical properties are concerned. Combining the data for 75 clusters with at least 20 member galaxies, they found that the line-of-sight velocity dispersion (with respect to the cluster mean velocity), σ_{los} , is $21 \pm 2\%$ larger for the ELG than it is for the non-ELG. They also found that the spatial distribution of the ELG is significantly less peaked towards the cluster centre than that of the non-ELG.

For a full appreciation of this result it is important to remember that the subsample of ELG consists almost exclusively of late-type galaxies, whereas the subset of non-ELG contains galaxies of all types. In other words: if the late-type galaxies without emission-lines would share the distribution and kinematics of their ELG counterparts, the differences between early- and late-type galaxies could well be more pronounced than between non-ELG and ELG.

On the other hand, it is also quite possible that the less centrally-concentrated distribution and larger σ_{los} apply only to the late-type galaxies *with* emission lines. If so, that would provide additional support for the conclusion in Paper III that the ELG are likely to be on fairly radial, first-approach orbits, as suggested by their larger velocity dispersion, their projected spatial distribution, and their rather steep velocity dispersion profile $\sigma_{los}(r_{proj})$. The presence of the line-emitting gas would be fully consistent with this picture.

5.1. Kinematics

We have repeated part of the analysis of Paper III, making use of the classification in early- and late-type galaxies on the basis of the spectrum, discussed in this Paper. We start with the same set of 75 clusters as in Paper III. However, our galaxy sample includes only those galaxies for which we could estimate the galaxy morphology from the PCA and ANN. This limits the sample to 2594 galaxies in 66 clusters, of which 399 galaxies are ELG, while 1571 ± 52 are classified as early-type, and 1023 ± 52 as late-type. For each galaxy the normalized line-of-sight component of the velocity w.r.t. the cluster centre, $v_{norm} = (v - v_{clus})/\sigma_{clus}$, is determined, where v_{clus} is the average cluster velocity and σ_{clus} is the line-of-sight velocity dispersion of the cluster to which the galaxy belongs. Following Paper III, we construct one large composite cluster by combining the data of all 66 clusters.

Using this sample of 2594 galaxies in 66 clusters, we find that the normalized line-of-sight velocity dispersion σ_{los} of the ELG is 23% larger than that of the non-ELG, which is fully consistent with the result of Paper III. The values of σ_{los} for ELG and non-ELG are given in column 3 of Table 5. The value of σ_{los} for the dominant class of non-ELG is larger than unity because, in constructing the composite cluster, one adds velocity distributions for which the average velocities are known only with a limited accuracy. This leads to the superposition of (approximately Gaussian) velocity distributions with small apparent offsets, which slightly increases the dispersion above the expected value of 1.00. As discussed extensively in Paper III, this effect certainly does *not* explain the value of σ_{los} of 1.28 for the ELG, because there is no evidence that the ELG have significant velocity offsets w.r.t. the non-ELG.

In Table 5 we also give the values of σ_{los} for several other subsets of the total sample. It appears that the σ_{los} of the late-type galaxies is $12 \pm 3\%$ larger than that of the early-type galaxies. This difference is significantly smaller than it is for ELG versus non-ELG, which makes it unlikely that the non-ELG spirals have the same kinematics as the ELG (mostly late spirals).

Table 5. Line-of-sight velocity dispersion (with respect to the cluster centre) and parameter values of the best-fitting β -model $\Sigma(r) = \Sigma(0) [1 + (r/r_c)^2]^\beta$ to the surface density profiles of galaxies. Column 1 gives the subsample of galaxies. Column 2 gives the number of galaxies in this subsample. All values are averages (\pm r.m.s. values around these averages) over 10 realizations of the ANN. The best-fitting model parameters are not listed for the early-type ELG, as these are very uncertain.

sample	N	σ_{los}	β	r_c
all	2594	1.08	-0.66	0.10
non-ELG	2195	1.04	-0.69	0.10
ELG	399	1.28	-0.67	0.27
early-type	1571 ± 52	1.03 ± 0.01	-0.66	0.08
late-type	1023 ± 52	1.15 ± 0.02	-0.76	0.23
early-type				
non-ELG	1504 ± 51	1.02 ± 0.01	-0.70	0.09
ELG	67 ± 24	1.22 ± 0.14	-	-
late-type				
non-ELG	691 ± 51	1.09 ± 0.03	-0.76	0.20
ELG	332 ± 24	1.28 ± 0.01	-1.24	0.71

This is indeed confirmed by the value of σ_{los} for the non-ELG late-type galaxies (mostly early spirals) of 1.09 ± 0.03 . Although this is somewhat higher than the value of 1.04 for all non-ELG, it is also very much smaller than the value of 1.28 found for all ELG, and for the subset of late-type ELG.

The intermediate value of 1.09 ± 0.03 for the non-ELG late-type galaxies may mean one of three things. First, and most simply, it may be a statistical fluke, i.e. a 2σ excursion of a value that is not fundamentally different from the 1.03 ± 0.01 that we find for the early-type galaxies. Secondly, the separation of the late-type galaxies into ELG and non-ELG may not be perfect. This could be a result of our observational limit for the detection of emission lines, which need not correspond exactly to a kinematical distinction. In other words: the non-ELG late-type galaxy category may contain a fraction (which must be significant) of intrinsic ELG, for which the emission lines were not detectable in the ENACS. In that case, the true σ_{los} of the non-ELG late-type galaxies is smaller and closer to the value of 1.03 ± 0.01 found for the early-type galaxies. Thirdly, the non-ELG late-type galaxies may be a dynamically ‘pure’ class, with kinematics intermediate between that of the early-type galaxies and that of the late-type ELG.

One might have a slight worry that the results in Table 5 are somewhat influenced by the fact the separation between e.g. early- and late-type galaxies on the basis of the spectrum is not perfect. In other words: the value of σ_{los} for the early-type class may have been somewhat overestimated because the early-type class contains a non-negligible contribution of late-type galaxies. Similarly, the value of σ_{los} for the late-type class may be somewhat underestimated. However, these effects are small.

Using the success rates in Table 3 for the two-class system, we estimate that at most 1 out of 4 galaxies in the early-type class is a misclassified late-type galaxy. Because essentially all galaxies in the early-type class (i.e. including the misclassified late-type galaxies) are non-ELG, the value of σ_{los} of the early-type class is not overestimated very much. Using the value of σ_{los} of 1.09 for the late-type non-ELG galaxies (which is a slight underestimate, see below), we estimate the bias in σ_{los} of the non-ELG early-type galaxies to be at most a few percent. With this result, we can estimate that the value of σ_{los} of the late-type non-ELG is more likely to be about 1.13 rather than 1.09, but this is still considerably smaller than the value of 1.28 of the late-type ELG.

Therefore, the data in Table 5 support a picture in which there is a clear correlation between the presence of emission lines and a high velocity dispersion. Rather unexpectedly perhaps, the ratio between the σ_{los} of ELG and that of non-ELG does not appear to depend on whether the ELG or non-ELG are early- or late-type galaxies. The ELG among the early- and late-type galaxies have a value of σ_{los} that is about 18% larger than that of the non-ELG of the corresponding galaxy type. In view of the large uncertainty in the estimate of σ_{los} for the early-type ELG, this may be totally fortuitous, however, and we certainly should not overinterpret this result.

In summary, the basic factor driving the difference in kinematics seems to be the presence or absence of emission lines, whereas the distinction between early- and late-type galaxies is less important, while the class of late-type non-ELG presents an intriguing cross-breed which may hold important clues to the physical meaning of the results.

5.2. Projected distributions

In view of the results in Table 5 and in Paper III, it is interesting to see how the kinematics and the projected spatial distribution are related. We therefore determined the surface density profiles of all subsamples, which we show in Fig. 6. The profiles are averages over the 10 realizations of the ANN (for the samples based on the distinction between early- and late-type). The profiles are shifted vertically such that at $r = 1h^{-1}$ Mpc the fitted profiles have the same values. The lines show the best-fitting β -model,

$$\Sigma(r) = \Sigma(0) [1 + (r/r_c)^2]^\beta \quad (1)$$

where Σ is the surface density, r_c is the core-radius and β is the logarithmic slope at large radii. The best-fitting values of β and r_c are given in columns 4 and 5 of Table 5. Note that, as a result of the details of the OPTOPUS observations, the spatial completeness of the galaxy samples may not be uniform, so that the estimate of β may be biased. The errors in the estimates, determined from the comparison of the 10 realizations of the ANN, are small, of the order of 10%. Only for the early-type ELG the errors are substantially larger because the number of galaxies in this subsample is small.

The non-ELG are significantly more centrally peaked than the ELG, as was already concluded by Biviano et al. Although

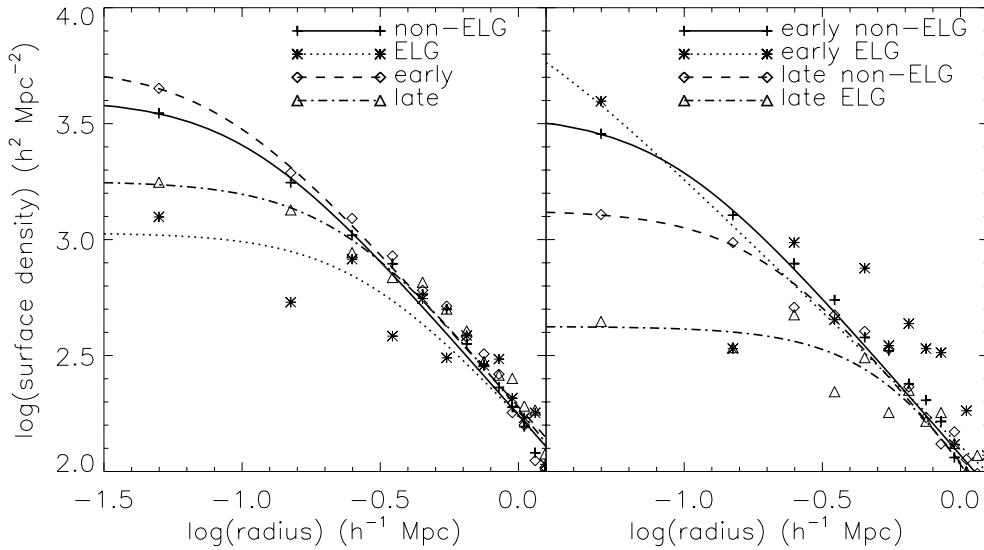


Fig. 6. Surface density profiles for the various subsamples of galaxies. The lines are the best-fitting β -models. The parameters of these are listed in Table 5.

we find the same value of β for both subsamples, the ELG population has a much larger core-radius r_c than that of the non-ELG. The difference between early- and late-types is similar to that between non-ELG and ELG, the former being more centrally concentrated than the latter. The subsample of late-type ELG has a value of β that seems different from that of all other subsamples, but the difference probably is not significant, as r_c is quite large.

Apparently, the late-type ELG are distributed much more towards the cluster outskirts than all other galaxies, including the late-type non-ELG. For the early-type ELG, the values of β (-0.58) and r_c (0.02) are not very reliable because of the small number of galaxies involved. However, from a comparison between all ELG and the late-type ELG, one may conclude that both β and r_c are probably quite small for the early-type ELG. So the distribution of early-type ELG probably also deviates from that of the other galaxies, in the sense that they are more centrally concentrated. As we have seen in Sect. 4.2, the early-type ELG are often AGN, and this result therefore is not too surprising.

However, the early-type ELG may also contain a contribution from central dominant galaxies with emission lines from cooling flows (e.g. Heckman et al. 1989, and Crawford et al. 1995), which might give an important contribution to the high surface density of early-type ELG in the innermost bin in Fig. 6. Yet, it is not clear that the line ratios of the lines we observe are consistent with this explanation, and from our present data it is not easy to estimate this contribution.

5.3. What does it mean?

Combining the results of the spatial and kinematical properties of the different galaxy populations, we conclude that the late-type non-ELG have properties that resemble more those of the early-type galaxies, i.e. most of the other non-ELG. Yet, their projected distribution is slightly wider than that of the early-type galaxies, with a core radius that is a factor two to three larger,

and kinematically they are somewhat ‘hotter’ than the other non-ELG. The (late-type) ELG, which consist mostly of spirals, behave very differently. Their line-of-sight velocity dispersion σ_{los} is much larger than that of the late-type non-ELG and they are located more towards the outer regions of clusters.

In Paper III the kinematical characteristics of ELG and non-ELG were interpreted as an indication for the ELG to be mostly on fairly (but not necessarily purely) radial orbits, in contrast to the non-ELG. Combining this with the larger velocity dispersion of the ELG and their relative scarcity in the very central regions of the clusters, we were led to the hypothesis that the ELG are mostly on radial, first-approach infall orbits towards the central regions of their clusters. This would be consistent with the presence of the line-emitting gas, as it is likely that that would have been removed from the galaxy on traversing the dense cluster core.

When the ELG are on orbits which are sufficiently radial without, however, traversing the very central regions, it is possible that they have already made several crossings without losing their gas, and will continue to do so until they ‘get caught’. In other words: their high velocity dispersion need not necessarily imply ‘first approach’ orbits, because in the absence of an encounter they could maintain their velocity, which was due to their ‘late’ infall. We may assume that an ELG which gets too close to the cluster centre (either on its first approach or after several crossings) will probably be ‘converted’ almost instantly into a non-ELG late-type galaxy, as the gas gets stripped.

How the gas gets stripped from the ELG is not totally clear. In principle, ram pressure against intracluster gas could do the trick. However, that probably would not change the kinematics and distribution of the left-overs as drastically as observed. Alternatively, the harassment of galaxies through fairly high-speed and relatively distant encounters, as described by Moore et al. (1996), could be responsible for driving out the gas. Such encounters could be sufficiently frequent (about once per Gyr) to ensure that gas-rich ELG are virtually absent from the central

regions. Actually, it is possible that an ELG has to experience a few of those encounters to get rid of its gas.

However, it is not immediately clear that such encounters will ‘instantly’ reduce their velocity dispersion of 1.28 to 1.09, the value observed for their non-ELG counterpart. One factor which may contribute to this large apparent reduction is projection. If the ELG are indeed on fairly radial orbits, and their gas-robbed encounter products are on less radial orbits, this geometric effect might be responsible for most of the apparent reduction of σ_{los} .

Thus, it is possible that a slight change of the orbit characteristics (in particular the anisotropy parameter \mathcal{A}), which results from the encounter which strips the ELG from its gas, is sufficient to considerably reduce σ_{los} and produce a more centrally concentrated distribution. Note, however, that the kinematics and distribution of these stripped ELG may be different from those of the early-type galaxies which suggests that the latter are a more advanced product of encounters in the central cluster region.

The AGN among the ELG are a special class. They are predominantly ellipticals which, probably because of their central location, show AGN characteristics. Our data unfortunately do not allow us to determine convincingly how their velocity dispersion compares to those of the other types of galaxies in the cluster (see Table 5), but they seem to be at least as centrally concentrated as the non-AGN early-type galaxies.

6. Summary and conclusions

We studied the spatial and kinematical properties of early- and late-type galaxies in a subset of the rich Abell clusters observed in the ENACS. We compared these properties for galaxies with emission lines (ELG) and without (non-ELG).

As for only about 10% of the galaxies in the ENACS the morphological type was known from imaging, we applied a Principal Component Analysis (PCA) in combination with an Artificial Neural Network (ANN), to try and classify all galaxies in the ENACS on the basis of their spectrum. The PCA is an important first step in the classification as it compresses essentially all significant information of a spectrum into a limited number of Principal Components (PCs).

These PCs, which are linear combinations of the original spectral fluxes, were subsequently used in an ANN. The ANN was trained to classify spectra using a subset of 150 galaxies for which the morphological type is known (D80). Another 120 galaxies for which the morphology is available from D80, the so-called test set, were used to determine the success rate of the classification algorithm.

Classifying galaxies into three classes (E, S0 and S+I), the ANN yielded the correct galaxy morphology of D80 for $49 \pm 6\%$ of the galaxies in the test set. The success rate increased to $73 \pm 4\%$ when the galaxies were classified into only two classes, early- (E+S0) and late-type (S+I) galaxies. Furthermore, $80 \pm 7\%$ of the galaxies with emission lines in their spectrum (ELG) was classified as late-type. This fraction is larger than the $58 \pm 5\%$ that one expects from the individual success

rates for each morphological type separately. Apparently, the success rate for the ELG is larger than for the entire set of galaxies.

We discussed several factors that may produce misclassifications. First, one does not always know the *true* galaxy type. Using galaxies which Dressler classified twice, we estimate that at least between 5 and 10% of the classifications based on imaging are incorrect. Secondly, even within one morphological type the spectra may be substantially different. Thirdly, S0 galaxies may be hard to separate from ellipticals from their spectrum alone, and we find that a rather large number of E’s is classified as S0 and vice versa, whereas the number of misclassifications between S0 and S+I is much smaller. Finally, spiral galaxies with a large bulge may have a spectrum that leads to a bona-fide early-type classification with PCA and ANN.

We investigated how galaxies of different type are distributed in the plane defined by the two most significant PCA components. There appears to be a distinction between E, S0 and S+I galaxies in this plane, although it is not very large. On the contrary, the ELG and non-ELG have clearly different distributions, which shows that the PCs contain significant information about the morphological type of a galaxy.

Finally, we extended the analysis of Biviano et al. (in Paper III), who studied the differences in the spatial and kinematical properties of ELG and non-ELG, to galaxies of different morphology. We conclude that the presence of emission lines, rather than the galaxy morphology, is the basic property that is correlated with the spatial and kinematical properties of a galaxy. Thus, the correlation between morphology on the one hand and spatial and kinematical properties on the other hand seems to result mainly, if not exclusively, from the presence of emission lines.

The line-of-sight velocity dispersion with respect to the average cluster velocity is larger for the ELG than it is for the non-ELG, and. A similar, but smaller, difference is found between late- and early-type galaxies. This supports the idea that the ELG are on fairly radial, and possibly ‘first approach’ orbits towards their cluster centres, while their line-emitting gas has not yet been stripped. In addition, the late-type galaxies *without* emission lines (i.e. with little gas) appear to have spatial and kinematical properties that more resemble those of the early-type galaxies than those of the late-type galaxies *with* emission lines. Apparently, if a late-type galaxy has passed through the cluster centre, most of its gas will have been stripped and the galaxy will not show emission lines anymore.

Acknowledgements. We thank Simon Folkes, Ofer Lahav and Avi Naim for valuable discussions and suggestions. Ben Kröse is acknowledged for a stimulating discussion, and Richard Arnold for triggering our interest in Artificial Neural Networks. We thank the ENACS team for allowing us to use the data, and Jaime Perea in particular for comments about the spectral reduction.

References

- Bailer-Jones C.A.L., 1997, PASP 109, 932
- Biviano A., Katgert P., Mazure A., et al., 1997, A&A 321, 84 (Paper III)

- Bromley B.C., Press W.H., Lin H., Kirschner R.P., 1998, *ApJ* 505, 25
Carlberg R.G., Yee H.K., Ellingson E., et al., 1996, *ApJ* 462, 32
Colless M., Dunn A.M., 1996, *ApJ* 458, 435
Connolly A.J., Szalay A.S., Bershadsky M.A., Kinney A.L., Calzetti D., 1995, *AJ* 110 1071
Crawford C.S., Edge A.C., Fabian A.C. et al., 1995, *MNRAS* 274, 75
Deeming T.J., 1963, *MNRAS* 127, 493
de Villiers J., Barnard E., 1993, *IEEE Trans. on Neural Networks*, 4, 136
Dressler A., 1980, *ApJS* 42, 565 (D80)
Folkes S.R., Lahav O., Maddox S.J., 1996, *MNRAS* 283, 651 (FLM96)
Francis P., Hewett P.C., Foltz C.B., Chafee F.H., 1992, *ApJ* 398, 476
Galaz G., de Lapparant V., 1998, *A&A* 332, 459
Heckman T.M., Baum S.A., van Breugel W.J.M., McCarthy P., 1989, *ApJ* 338, 48
Hertz J., Krogh A., Palmer R.G., 1991, In: *Introduction to the theory of neural computation*. Addison Wesley, Redwood City, California
Ibata R.A., Irwin M.J., 1997, *AJ* 113, 1865
Katgert P., Mazure A., Perea J., et al., 1996, *A&A* 310, 8 (Paper I)
Katgert P., Mazure A., den Hartog R., et al. 1998, *A&AS* 129, 399 (Paper V)
Kendall M.G., Stuart A., 1968, *The Advanced Theory of Statistics*. Charles Griffin & Company Limited, London
Kröse B.J.A., van der Smagt P.P., 1993, *An Introduction to Neural Networks*. University of Amsterdam
Lahav O., Naim A., Sodr e Jr. L., Storrie-Lombardi M.C., 1996, *MNRAS* 283, 207
Lauberts A., Valentijn E.A., 1989, *The Surface Photometry Catalogue of the ESO–Uppsala Galaxies*. ESO
Mohr J.J., Geller M.J., Fabricant D.G., et al., 1996, *ApJ* 470, 724
Moore B., Katz N., Lake G., Dressler A., Oemler A., 1996, *Nat* 379, 613
Naim A., Lahav O., Buta R.J., et al., 1994, *MNRAS* 274, 1107
Naim A., Lahav O., Sodr e Jr. L., Storrie-Lombardi M.C., 1995, *MNRAS* 275, 567
Ram rez A.C., de Souza R.E., 1998, *ApJ* 496, 693
Singh H.P., Gulati R.K., Gupta R., 1998, *MNRAS* 295, 312
Sodr e Jr. L., Cuevas H., 1994, *Vistas in Astronomy* 38, 287
Sodr e Jr. L., Cuevas H., 1997, *MNRAS* 287, 137
Storrie-Lombardi M.C., Lahav O., Sodr e Jr. L., Storrie-Lombardi L.J., 1992, *MNRAS* 259, 8p
von Hippel T., Storrie-Lombardi L.J., Storrie-Lombardi M.C., Irwin M.J., 1994, *MNRAS* 269, 97
Weaver W.B., Torres-Dodgen A.V., 1997, *ApJ* 487, 847
Zaritsky D., Zabludoff A.I., Willick J.A., 1995, *AJ* 110, 1602